large (e.g., for the $l=4$ partial wave in Cm^{242} alpha decay).

VI. SUMMARY

Through approximate methods we are able to obtain information concerning the alpha decay of deformed nuclei which was heretofore obtainable only through detailed numerical integrations. We have developed approximate methods for calculating both alpha partial-wave amplitudes at the nuclear surface and phase shifting caused by nuclear quadrupole deformation.

PHYSICAL REVIEW VOLUME 112, NUMBER 2 OCTOBER 15, 1958

Precision Determination of Nuclear Energy Levels in Heavy Elements*

E. L. CHUPP, J. W. M. DUMOND,† F. J. GORDON, R. C. JOPSON, AND HANS MARK‡
Radiation Laboratory, University of California, Livermore, California

(Received April 17, 1958)

The low-lying energy levels in 32 isotopes between $Z=62$ and $Z=75$ have been studied using a high-precision bent quartz crystal spectrograph to determine gamma-ray energies. The gamma rays were produced by the electric (or Coulomb) excitation process. The high proton-beam current of the A-48 accelerator was used to provide the intense sources necessary for these experiments. With this technique, energies in the 100-kev region can be determined with a precision of about one part in 2000. A comparison of the results with the unified model of nuclear structure is given.

I. INTRODUCTION

IN a previous paper,[1] a technique for determining the energies of low-lying levels in heavy nuclei with high precision was described. The present work is an account of the subsequent extension and development of this method. Since substantial changes in experimental procedure and data analysis have been made in the time since the first publication, a short recapitulation of the method is in order.

For nearly five years the electromagnetic (or Coulomb) excitation process[2] has been a very useful tool for the study of nuclear energy levels near the ground state. There are several reasons why electromagnetic excitation is well suited for this purpose:

(1) The cross section is large (of the order of several millibarns for many heavy elements at the proton energy available) and there are no background effects (neutrons or high-energy capture gamma rays) which would complicate the detection of the resulting nuclear gamma rays.

(2) The excitation cross section is related to the transition rate (or partial transition rate in the case of mixed transitions) of the nuclear excitation. It is therefore possible in one experiment not only to establish the existence of an energy level but also to learn something about the matrix elements which determine the transition rates.

The large gamma-ray yields from electric excitation reactions and the high beam currents available from the A-48 accelerator (UCRL, Livermore) provide effective source strengths of several hundred millicuries. With such sources, it is possible to employ a high-precision bent quartz crystal spectrograph to analyze the gamma rays. It is therefore possible to determine the wavelengths (and energies) of many electric excitation gamma rays with a precision ranging from one part in 3000 for low energies ($\sim$50 kev) to one part in 1000 for higher energies ($\sim$150 kev). No attempt was made in these experiments to determine excitation cross sections since the efficiency of the bent crystal spectrograph is a very strong function of the gamma-ray energy.[3] The proper response curve for the instrument would have to be determined with great accuracy if cross-section measurements more accurate than the best ones available now[4] are to be made. In addition, accurate methods of measuring high beam currents would have to be developed. In view of these facts it was decided to concentrate exclusively on determining the energies of as many levels as possible as accurately as possible.

Aside from the intrinsic value of making measurements that are more precise than those available at present, there are several reasons why accurate determinations of energies of low-lying nuclear levels in the heavy elements are important. In heavy elements (beginning around $Z=60$) the first few energy levels belong to the rotational band of the ground state. The theory of nuclear structure developed by Bohr and his

* Work done under the auspices of the U. S. Atomic Energy Commission.

† California Institute of Technology, Pasadena, California.
‡ Massachusetts Institute of Technology, Cambridge, Massachusetts.

[1] Chupp, Clark, DuMond, Gordon, and Mark, Phys. Rev. **107**, 745 (1957).

[2] Alder, Bohr, Huus, Mottelson, and Winther, Revs. Modern Phys. **28**, 432 (1956).

[3] Lind, West, and DuMond, Phys. Rev. **77**, 475 (1950).

[4] N. P. Heydenburg and G. M. Temmer, *Annual Review of Nuclear Science* (Annual Reviews, Inc., Palo Alto, 1956), Vol. 6, p. 77.

collaborators[5] makes predictions which require accurate energy-level measurements for verification. For example, in odd-A isotopes, the Coulomb excitation process populates the first two rotational levels, thereby making it possible to verify the well-known rotational level sequence in these cases. Precision measurements of rotational spectra reveal small deviations from the rotational level sequence arising from small higher order terms in the Hamiltonian of the collective model.[5] These deviations are so small ($\sim$0.5 to 1% in most cases) that it has not been possible to detect them in a statistically significant way without the use of a bent crystal γ-ray spectrograph or precision α- or β-ray spectrometers. Because of the present methods, statistically significant deviations from the rotational interval rule have been found in three isotopes (Ta^{181}, Ho^{165}, and Tb^{159}). (See Sec. IV.)

In even-A isotopes, only the first rotational level can be excited with sufficient intensity to make precision measurements feasible. It is therefore not possible to study level sequences in individual isotopes. However, the position of the first excited level in a series of neighboring isotopes measured as a function of A or neutron number is interesting, since this energy is related to the nuclear deformation in this region of the periodic table. In several cases, neighboring even-A isotopes (Er^{166}, Er^{168}, Er^{170} and Hf^{178}, Hf^{180}, etc.) have first excited levels so close together that they can only be resolved by the use of precision methods.

There is still another reason why high resolution is important. Whenever an electric excitation experiment is performed the characteristic K x-rays of the bombarded material are detected along with any gamma rays that may be present. In several rare-earth isotopes there are nuclear levels and K x-rays in the same region (between 50 and 60 kev). In a scintillation counter experiment, these gamma rays cannot be resolved from the K x-rays; therefore their presence can only be inferred from changes in the K x-ray yield.[6] With the resolution of the bent crystal spectrograph it is possible to separate the nuclear and atomic excitations for these isotopes. Several cases of this type will be discussed.

II. EQUIPMENT AND PROCEDURE

The A-48 high-current linear accelerator[7] has several properties which make it an ideal machine for electric excitation experiments. The maximum proton energy is 3.7 Mev, which is below the Coulomb barrier energy for elements with $Z>60$. The background radiation near the accelerator is not excessive, which means that no abnormal measures are necessary to protect the detector. Finally, the machine operates very reliably at proton gradient; hence, the relatively long ($\sim$50-hour) bombardments necessary for the electric excitation experiments were made practically without interruption. A drawing of the experimental arrangement is shown in Fig. 1. The spectrograph is mounted on a shockproof platform suspended from the heavy concrete shield wall so that line broadening from vibrations is minimized.

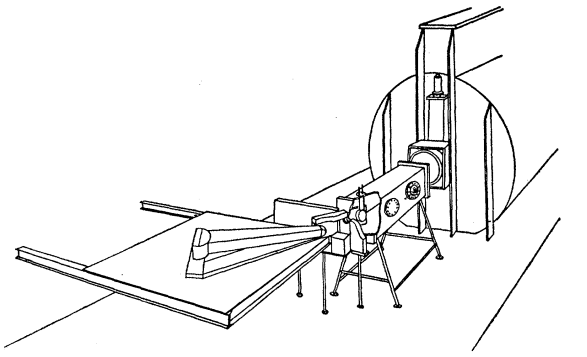

FIG. 1. Drawing showing the position of the accelerator, target, spectrograph, and shockproof platform.

A principal limitation on the maximum beam current available from the A-48 is the heat load that can be put on the target. The standard probe consists of a 4×7 inch metal plate ($\frac{1}{8}$ to $\frac{1}{4}$ inch thick) mounted in such a way that a high-pressure water flow of between 10 and 30 gallons per minute is maintained across the back of the probe. On copper plates it is possible to dissipate $\sim$20 kw per square inch in this manner. Since the beam has an area of about 4–5 sq. in., the power developed at the target is $\sim$100 kw, which means that proton beam currents of the order of 25 milliamperes can be put on such copper plates. In practice, most targets could not stand such large heat loads, since most materials have a smaller thermal conductivity than copper; therefore, the usual beam currents used in most of these experiments were between 2 and 5 milliamperes. The beam currents were determined by measuring the temperature rise in the cooling water and the water flow and then converting this to power dissipated on the target. This method of measuring the beam current is probably accurate to about 15%.

Several different types of targets were used in the course of these experiments. Some of the materials could be used as plates, $\frac{1}{8}$ to $\frac{1}{4}$ inch thick and large enough to be mounted directly on the probe holders. Uranium, thorium, platinum, and tantalum were bombarded in this manner. It was found that platinum and tantalum make satisfactory targets since their heat conductivities are relatively large, whereas uranium and thorium are very poor target materials since their heat conductivities are exceedingly small. The uranium probe could not stand beam currents larger than 0.4 ma. Another method used for making probes was to

[5] A. Bohr, Kgl. Danske Videnskab. Selskab, Mat.-fys. Medd. **26**, No. 14 (1952); A. Bohr and B. R. Mottelson, Kgl. Danske Videnskab. Selskab, Mat.-fys. Medd. **27**, No. 16 (1953), and several subsequent papers.

[6] N. P. Heydenburg and G. F. Pieper, Phys. Rev. **107**, 1297 (1957).

[7] E. O. Lawrence, Science **122**, 1127 (1955).

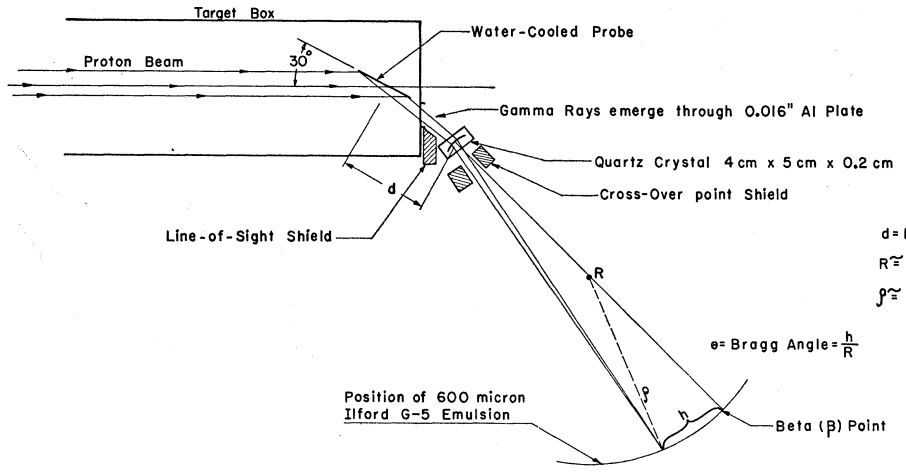

FIG. 2. Experimental geometry.

solder a thin sheet of the material to be bombarded to a copper backing plate. This technique was used for the gold, rhenium, and hafnium targets. The gold and hafnium targets were quite satisfactory but rhenium proved to be difficult to solder to copper, which resulted in the probe being burned through in several places where there was no thermal contact between the rhenium and the copper.

A large number of the materials studied were not available in quantities large enough to make use of the methods of the preceding paragraph for manufacturing target probes. With two exceptions (erbium and gadilinium) the rare-earth metals were available only in ~10-gram lots, so that a different method of making targets had to be developed. Most of the rare earths (in metallic form) are quite easy to evaporate (boiling point is around 2000°C). It was found that satisfactory targets could be made by depositing thin layers of these materials on copper backing plates. These targets could be bombarded with beams up to 3 ma; although in some cases the evaporated layer apparently was not in good thermal contact with the backing plate and consequently burned off as soon as the beam was turned on. In addition, if the rare-earth layer was not thick enough, background radiation from the copper contributed to fogging the photographic plate on which the spectrum was recorded. The principal reaction contributing to this background is $Cu^{65}(p,n)Zn^{65}$ which has a threshold of about 2 Mev. If the evaporated layer was so thin that the 3.7-Mev protons did not lose at least 1.7 Mev in traversing the layer, or if the layer was burned through in several places, neutrons were emitted at the target. Capture gamma rays from these neutrons and proton recoil tracks in the emulsion darkened the plate. If any substantial increase in the neutron background counting rate was noted during a run, a new target was installed. With the evaporation geometry used in these experiments, successful targets could be made with about two grams of the rare-earth metal. The amount of material deposited on the 12.5-in.^{2} target was usually between 0.5 and 1 gram.

On several rare-earth spectral plates, which were made using evaporated targets, certain gamma-ray lines ($E=54$ kev, 61 kev, and 115 kev) were always observed (see Table IV). These lines could not come from the rare earths in question, since it is highly unlikely that five or six isotopes have levels at precisely the same energy. Further investigation revealed that these lines resulted from the $Cu^{65}(p,n,\gamma)Zn^{65}$ reaction in the copper backing, which occurred if the rare-earth layer was not thick enough to stop the protons. The cross section for this process[8] is large enough (~50 mb) so that the gamma rays can be recorded on the plate before it is severely darkened by the neutron background. Energy levels in several other light elements were studied in this manner and will be the subject of a separate report.

The bent quartz crystal spectrograph used in these experiments has been thoroughly discussed in reference 1 and also in previous articles.[9] The geometry—including the various shields for the photographic recording instrument (Cauchois type)—is shown in Fig. 2. The 4×5×0.2 cm quartz crystal is bent by the stainless steel holder along an arc with a radius of 2 meters such that the (310) planes in the crystal point to a spot (β point) 2 meters from its concave surface. If a source is placed at the position indicated in Fig. 2, then the different wavelengths will be focused at different points along a focal circle with a one-meter radius. The lines were recorded on photographic plates which consisted of 600 micron Ilford G-5 nuclear emulsions mounted on 30-mil glass plates. The glass plates were 10 in. long so that the lowest energies which could be observed were of the order of 30 kev. The original

[8] E. M. Bernstein and H. W. Lewis, Phys. Rev. **107**, 737 (1957).
[9] J. W. M. DuMond, in *Ergebnisse der Exakten Naturwissenschaften* (Springer-Verlag, Berlin, 1955), Vol. 28, p. 232.

reasons for choosing this method of detection are given in reference 1.

The "resolution" of the bent crystal spectrograph used in these experiments is defined as $\delta\lambda/\lambda$ where $\delta\lambda$ is the full "width" of the line on the plate and λ is the wavelength of the line. The average width of a nuclear line is 0.20 mm which corresponds to a $\delta\lambda$ of approximately 0.24 mA. For a gamma-ray energy of 100 kev ($\lambda = 123.7$ mA), one has

$$\delta\lambda/\lambda \quad \text{and} \quad \delta E/E = 2.0\times10^{-3}.$$

This result means that at 100 kev, two lines that are separated in energy by 200 electron volts will not overlap. It should be pointed out that the resolution is not the same as the standard deviation of the energy measurement, since it is possible to determine the position of the center of a line on the plate more accurately than 0.20 mm. This point is discussed in greater detail in Sec. III.

The shielding of the photographic plate is extremely important since it ultimately determines the over-all signal-to-noise ratio for the experiment. The principal shields are shown in Fig. 2. The function of the "line-of-sight" shield between the source and the crystal is to protect the emulsion from radiations starting at the source which are not reflected by the crystal planes. This shield is placed so that no direct radiations can reach points on the film beyond the β point. The second shield designed to prevent fogging due to undiffracted radiations is the "cross-over-point" shield. The effective width of the source in most experiments is about $\frac{1}{4}$ in., which is only about 15% of the aperture of the crystal. Short-wavelength radiations having small Bragg angles will be diffracted by the portion of the crystal nearest the "line-of-sight" shield, and those with long wavelengths will be diffracted at the other end of the crystal. Since the long-wavelength lines are farther from the β point than the short-wavelength lines on the photographic plate, the "rays" corresponding to different wavelengths must "cross over" at some point behind the crystal. This "cross-over point" is about 20 cm behind the crystal and all the diffracted "rays" at this point form a bundle that is not much wider than the source. The "cross-over point" shield is then placed in such a way as to let through the diffracted bundle and shield all direct (undiffracted) radiations from the source which would reach the film by paths outside the region of the bundle of diffracted rays.

In addition to the "geometric" shielding mentioned in the last paragraph, a certain amount of general shielding against gamma rays and neutrons coming from places other than the target is necessary to protect the plate camera from scattered gamma rays. The lead tunnel, shown in Fig. 1, considerably reduced the solid angle available to background radiations that might strike the emulsion. The camera was, in addition, surrounded with a 4-inch layer of lead bricks. (The radiation level 1 meter from the target is usually about 100 mr per hour for a high-Z material target and a beam of $\sim$2 ma. This radiation level is sufficient to darken a plate after an exposure of the order of one hour.) In addition to the gamma-ray shield, a layer of 4 to 6 inches of pressed boric acid was placed around the plate camera in order to moderate and attenuate the scattered neutrons incident on the plate.

One important point that has not been explicitly discussed is the efficiency as a function of quantum energy of the bent crystal spectrograph used in the Cauchois geometry. The efficiency is defined as the ratio of the number of gamma quanta absorbed in a particular line on the nuclear emulsion to the number of quanta of that energy emitted by the source in all directions. Lind, West, and DuMond[3] have defined an integrated reflection coefficient, R_θ, as the equivalent angular range (around the Bragg angle) over which the crystal has a reflectivity of 100%. The integrated reflection coefficient essentially determines the solid angle into which an atom in the source must radiate in order that the radiation be selectively reflected by the crystal planes. The integrated reflection coefficient for the (310) planes in a bent quartz crystal 1 mm thick has been determined experimentally as a function of quantum energy.[3] For the crystal used in the present work, these numbers must be multiplied by 2 since the crystal thickness is 2 mm. Using the data of reference 3, the integrated reflection coefficient for the 2-mm crystal is

$$R_\theta = 3.5\times10^{-2}/E_\gamma^2, \tag{1}$$

where E_γ is the quantum energy in kev. In the Cauchois geometry shown in Fig. 2, the effective solid angle presented by the crystal at the source is

$$\Omega = dR_\theta h/d^2 = R_\theta h/d, \tag{2}$$

where d is the distance from the source to the crystal and h is the usable vertical height of the crystal. The ratio of the number of photons of energy E_γ emitted into a line to the total number of photons of the same energy emitted by the source is

$$N/N_0 = \Omega/4\pi = 1.1\times10^{-4}/E_\gamma^2, \tag{3}$$

where $d = 50$ cm and $h = 2$ cm have been used to evaluate the solid angle. The total efficiency of the spectrograph at this photon energy is this ratio multiplied by the efficiency of the detection device.

A 600-micron Ilford G-5 nuclear emulsion was used to record the gamma rays. The efficiency of this emulsion can be estimated using the data on emulsions given by Goldschmidt-Clermont[10] and the gamma-ray absorption cross-section measurements of Davisson and Evans.[10] If it is assumed that only the silver in the emulsion is effective in absorbing gamma rays, then a

[10] Y. Goldschmidt-Clermont, *Annual Review of Nuclear Science* (Annual Reviews, Inc., Palo Alto, 1953), Vol. 3, p. 141; and C. M. Davisson and R. D. Evans, Revs. Modern Phys. **24**, 79 (1952).

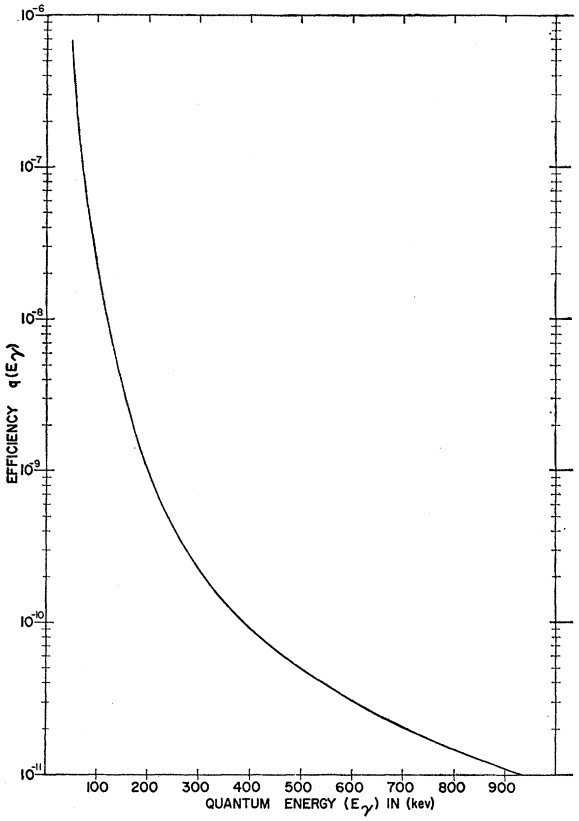

FIG. 3. Efficiency of bent quartz crystal spectrograph as a function of quantum energy. A factor of 4π was omitted in computing the ordinate of this curve. The correct efficiency is therefore given by the ordinate divided by 4π.

good approximation for the efficiency function of the emulsion in the region of a few hundred kev is

$$\epsilon=0.06\left[\frac{2.56\times10^6}{E_\gamma^3}+\frac{1}{E_\gamma^{\frac{1}{2}}}\right]. \quad (4)$$

The total efficiency of the spectrograph is then

$$q(E_\gamma)=\frac{N}{N_0}\epsilon=\frac{6.7\times10^{-6}}{E_\gamma^2}\left[\frac{2.56\times10^6}{E_\gamma^3}+\frac{1}{E_\gamma^{\frac{1}{2}}}\right]. \quad (5)$$

At a quantum energy of 100 kev, the efficiency of the spectrograph—that is, the ratio of the number of quanta absorbed by the detector at the focal circle to the number of quanta of that energy emitted by the source—is 1.4×10^{-9}. Figure 3 shows $q(E_\gamma)$ plotted against E_γ. The formula (5) is not valid for quantum energies below 40 kev since absorption effects in the crystal and in the air between the crystal and the film become important.

The practical upper limit of the quantum energies that can be studied with this spectrograph can be estimated from Fig. 3 and Eq. (5). At 100 kev, an exposure of 1 curie-hour is sufficient[11] to give a measurable line. At 1 Mev, the efficiency is lower by a factor of about 10^4, so that it is not possible to make measurements at this quantum energy unless extremely strong sources are used. In practice, for the experiments described in this and the preceding papers,[1,11] the upper limit of the quantum energy is between 150 and 200 kev. This upper limit can be raised considerably by using the bent crystal in the Mark I geometry.[9] The efficiency at high quantum energies is larger in this geometry because a high-efficiency detector (a large NaI crystal) can be easily employed. Furthermore, collimators can be constructed which make it possible to explore the spectrum close to the β point so that quantum energies up to 1.2 Mev can be measured. The drawback of this geometry for accelerator experiments is that it requires a line source rather than the extended one permissible in the Cauchois geometry, and this raises experimental problems that have not yet been solved. Equation (5) is a useful guide for estimating machine running times in order to observe certain lines. Examples of this will be given in Sec. IV.

The machine time necessary for the average target was of the order of 100 ma-hr, which at a beam level of about 2–3 ma means running times of the order of 30–50 hours. During the course of this work, the accelerator was operated for two shifts every day so that one spectrum was made every three or four days. The total number of plates (including repeats) that were made during the course of these experiments was 61, requiring a total exposure time of 5500 ma-hr and a running time of 200 days.

III. DATA REDUCTION AND ANALYSIS

The positions of all lines on a given plate were measured, relative to an arbitrary origin, with a high-precision optical comparator at the Astronomy Department of the University of California in Berkeley. This instrument has a screw travel length of 14 in. so that the 10-in. plate could be read without resetting. The line position was determined by setting the cross hairs first on the left and then on the right side of the line and the average of the two readings was taken as the line position. The smallest division on the comparator dial is one micron (10^{-3} mm) and repeated measurements of the center lines of a given line are reproducible to 20–30 microns. To account for distortion of the emulsion during development and to cancel any error in the position of the plate in the comparator, several (generally six) readings are made of the line position in different regions of the plate. The plate is then reversed in the comparator and the above procedure is repeated so that any systematic errors in the pitch of the screw are minimized. Twelve separate measurements of the position of most lines are therefore available.

[11] Chupp, DuMond, Gordon, Jopson, and Mark, Phys. Rev. **109**, 2036 (1958).

The bent crystal spectrograph used in the Cauchois geometry is well suited for determining the wavelengths of new gamma-ray lines relative to gamma-ray (or x-ray) lines of known wavelengths that also appear on the plate. (The reasons for not using this instrument to determine wavelengths *without* reference to other wavelength standards are discussed in reference 1.) In every bombardment of a target material with $Z>60$ the characteristic K shell x-rays of the element were recorded on the plate along with any nuclear gamma rays that may be present. Seven lines ($K_{\alpha 1}$, $K_{\alpha 2}$, $K_{\beta 1}$, $K_{\beta 2}$, $K_{\beta 3}$, $KO_{II}O_{III}$, and $K_{\beta 5}$) of the x-ray spectrum were readily visible on each plate. Since the wavelengths of some of these x-rays in all the elements considered have been measured with high precision, they are well suited for calibration purposes. In addition to the x-ray lines from the target, a set of lines from a strong (~one-curie) Ta^{182} source was put on each plate. The wavelengths of the gamma rays emitted by this source have been determined with high precision by one of us and his co-workers.[12] The Ta^{182} calibration exposures usually required a total exposure time of 30 hours. In order to detect any motion of the crystal or the emulsion during the machine run, the source exposures were carried out in two steps, one before the beginning and one after the conclusion of the machine exposure. The wavelengths of all the calibration lines used in the course of this work, together with the references to the original measurements of these wavelengths, are shown in Table I. The K_β x-rays were not used as calibration lines for the elements from $Z=62$ to $Z=72$, since the existing wavelength measurements of these lines are not as good as those of the K_α x-rays in the same elements (see reference a of Table I).

The method used for determining the wavelength of an unknown gamma-ray line with reference to the calibration lines on the plate have been discussed in references 1 and 11. In the present work, a somewhat different method has been adopted which makes the computation of the standard deviations of the measured wavelengths less difficult. The wavelength, λ, and the position, h, of a given line on the plate are related by the equation,

$$\arcsin(\lambda/2d)=(h-h_0)/R, \qquad (6)$$

where $2d$ is twice the spacing of the (310) planes in quartz ($2d=2355.34\pm0.04$ x units), h_0 is the position of the β point on the plate and R, the radius parameter of the spectrograph, is the distance between the center line of the quartz crystal and the β point. If n calibration lines are present on the plate, then a set of n equations of the type (6) in the unknowns R and h_0 can be written. Since n is always larger than 2, the set overdetermines R and h_0 so that a least-squares solution that gives the "best" values of these parameters must be carried out. Once R and h_0, together with their standard deviations and their correlation coefficient are determined for a given plate, then the wavelength, λ, and the standard deviation, $\sigma(\lambda)$, of any known gamma-ray line on the plate can be determined by substituting the position, h, of the unknown line into (6) and solving for λ.

[12] Murray, Boehm, Marmier, and DuMond, Phys. Rev. **97**, 1007 (1955).

TABLE I. Wavelengths of calibration lines used to determine the wavelengths of unknown gamma-ray lines.

Element	Line	Wavelength in Siegbahn x units	Reference
Sm	$K_{\alpha 2}$	313.20 ±0.03	a
	$K_{\alpha 1}$	308.54 ±0.03	a
Gd	$K_{\alpha 2}$	292.41 ±0.03	a
	$K_{\alpha 1}$	287.73 ±0.03	a
Tb	$K_{\alpha 2}$	282.94 ±0.03	a
	$K_{\alpha 1}$	278.19 ±0.03	a
Dy	$K_{\alpha 2}$	273.64 ±0.03	a
	$K_{\alpha 1}$	268.87 ±0.03	a
Ho	$K_{\alpha 2}$	264.99 ±0.03	b
	$K_{\alpha 1}$	260.30 ±0.03	b
Er	$K_{\alpha 2}$	256.72 ±0.03	a
	$K_{\alpha 1}$	251.99 ±0.03	a
Tm	$K_{\alpha 2}$	248.59 ±0.02	c
	$K_{\alpha 1}$	243.86 ±0.02	c
Yb	$K_{\alpha 2}$	240.99 ±0.02	c
	$K_{\alpha 1}$	236.22 ±0.02	c
Lu	$K_{\alpha 2}$	233.61 ±0.02	c
	$K_{\alpha 1}$	228.83 ±0.02	c
Hf	$K_{\alpha 2}$	226.61 ±0.02	c
	$K_{\alpha 1}$	221.81 ±0.02	c
Ta	$K_{\alpha 2}$	219.846±0.010	d
	$K_{\alpha 1}$	215.050±0.010	d
	$K_{\beta 3}$	190.492±0.010	d
	$K_{\beta 1}$	189.693±0.010	d
Re	$K_{\alpha 2}$	207.179±0.010	d
	$K_{\alpha 1}$	202.359±0.010	d
	$K_{\beta 3}$	179.323±0.010	d
	$K_{\beta 1}$	178.323±0.010	d
W	Gamma rays	188.259±0.018	e
	from nuclear	182.638±0.018	e
	levels in W^{182}	123.599±0.014	e

[a] J. M. Cork and B. R. Stephenson, Phys. Rev. **27**, 530 (1936).
[b] Y. Cauchois and H. Hulubei, *Longueurs d'Onde des émissions X et des discontinuités d'absorption X* (Herman et Cie, Paris, 1947).
[c] F. Boehm and E. N. Hatch (private communication).
[d] E. Inglestam, Nova Acta Regiae, Soc. Sci. Upsaliensis **4**, No. 5 (1936).
[e] Murray, Boehm, Marmier, and DuMond, Phys. Rev. **97**, 1007 (1955).

Several assumptions that were made in the computations considerably simplified the procedure outlined above. The same standard deviation (±0.01 mm) was assigned to all distance measurements on the plate. This number was chosen on the basis of a careful examination of the measurements made on a large number of lines. The first column in Table II shows the distance between the 68-kev and the 100-kev calibration lines on all the plates. It can be seen that in many cases the standard deviations are considerably less than ±0.01 mm. Small standard deviations in Δh[Ta(68 kev)-Ta(100 kev)] were obtained on those plates with intense, well-developed lines, which made it easy to position the cross hairs of the comparator microscope and the larger standard deviations occurred when the lines were less intense or when the plate was fogged by background radiations. The same standard deviation (±0.03 x units) was also assigned to all wavelengths used for calibration. This is also a conservative estimate

TABLE II. The distance between the 68-kev and 100-kev calibration lines on each plate is shown in the first column. The computed value of the spectrograph radius, R, obtained from the calibration lines on each plate is shown in the second column.

Plate	Δh[Ta(68 kev) − Ta(100 kev)] (in mm)	R (in mm)
$_{75}$Re	50.036±0.010	1991.9±0.8
$_{73}$Ta	50.042±0.003	1993.0±0.8
$_{72}$Hf	50.036±0.003	1992.2±0.7
$_{71}$Lu	50.014±0.005	1992.0±0.7
$_{70}$Yb	50.034±0.006	1991.8±0.7
$_{69}$Tm	50.038±0.004	1991.8±0.6
$_{68}$Er	50.026±0.005	1989.9±0.6
$_{67}$Ho	50.031±0.004	1991.2±0.6
$_{66}$Dy	50.047±0.004	1993.8±0.5
$_{65}$Tb	50.015±0.007	1991.2±0.5
$_{64}$Gd($\frac{1}{2}E$)	50.099±0.010	1992.3±0.5
$_{62}$Sm	50.038±0.009	1990.4±0.4

since many of the wavelengths listed in Table I have smaller standard deviations. If the assumptions outlined above are made, then the least-squares solution is simplified, since all the points (h_i,λ_i) have the same statistical weight. Since both of these error assignments are conservative, the standard deviations quoted in the measured wavelengths shown in Table III are *upper limits*.

Once the above assumptions were made, the least-squares solution for R and h_0 was carried out following the methods outlined in Chap. 11 of Worthing and Geffner[13] and Chap. 7 of Cohen *et al.*[14] The methods used for computing the standard deviations $\sigma(R)$ in R and $\sigma(h_0)$ in h_0 are also given in references 13 and 14. The second column in Table II shows the value of the spectrograph radius, R, obtained for each plate. The largest standard deviations in R occur when the calibration lines on a plate are near each other. (On the Re plate the distance between the Ta $K_{\alpha 2}$ x-ray line and the 100-kev line from the Ta^{182} source is about 10 cm, whereas on the samarium plate the distance between the Sm $K_{\alpha 2}$ line and the same 100-kev line is about 20 cm.) The spectrograph radius was also measured directly with a set of accurately calibrated micrometers. The best value of R obtained from these measurements is 1990.5±0.5 mm, which is in reasonable agreement with the computed values shown in Table II.

The wavelength, λ, and the standard deviation, $\sigma(\lambda)$, of each unknown line were calculated using the appropriate values of R and h_0 for each plate. The energy in kev of each unknown gamma ray was obtained using:

$$E\ (\text{kev}) = 12372.44 \pm 0.16/\lambda\ (\text{x units}), \qquad (7)$$

where the conversion factor is taken from DuMond and Cohen.[15] Because of the large amount of data that had to be analyzed in the course of this work, all the computations described in this section were carried out on the IBM–650 digital computer at UCRL, Livermore.

IV. RESULTS

Seventeen elements were bombarded in the series of experiments that are the subject of this report. In order of decreasing Z, the materials investigated were uranium, thorium, gold, platinum, rhenium, tantalum, hafnium, lutetium, ytterbium, thulium, erbium, holmium, dysprosium, terbium, gadolinium, samarium, and neodymium. These elements have 48 stable isotopes with a natural abundance greater than 5%. All gamma rays observed in these experiments result from the electric excitation of the nuclei by the incident protons. For most of the isotopes studied, the thick-target yield of gamma rays in the 100-kev region is about 10^{-7} gamma rays per proton.[2] Most targets were bombarded with beam currents of the order of 3 ma so that effective sources of the order of 50 millicuries were produced. To obtain the required exposure of 1 curie-hour, it is therefore necessary to make bombardments lasting 20 and 30 hours which means machine exposures of the order of 100 ma-hr. These statements are only qualitatively correct, and longer exposures are necessary when the isotopic abundance of a given species is small or when the gamma-ray energy is much above 100 kev [see Eq. (5)]. There is a practical upper limit of about 600 ma-hr on the total exposure time, since the general background inside the shield wall when the machine is operating causes blackening of the nuclear emulsion in spite of the shielding around the plate.

On five of the seventeen good plates that were made, no nuclear gamma-ray lines were observed. These elements were uranium, thorium, gold, platinum, and neodymium. Uranium and thorium (i.e., U^{238} and Th^{232}) both have nuclear energy levels[16] at about 50 kev with a value of $\epsilon B(E2)$ of about 0.04, which would require an exposure time of the order of 300 ma-hr. Since both uranium and thorium make rather poor targets, such long exposures were not feasible. Each plate was exposed for 100 ma-hr in the hope that something might appear even in a shorter exposure, but no positive results were obtained. Similar computations can be made to show that gold and platinum are also marginal targets for such experiments. Neodymium is also a poor material for study since the excitation energies in the abundant isotopes are too large (~300 kev).

The results of all other experiments are listed in Table III. The wavelengths are listed in Siegbahn x-units, which are a factor of 1.00204 larger than milliangstroms.[14,15]

In each case, the best previous measurement for the energy of the level is given (when available), obtained by scintillation counter methods, internal-conversion electron spectrometry or bent crystal diffraction

[13] A. G. Worthing and J. Geffner, *Treatment of Experimental Data* (John Wiley & Sons, Inc., New York, 1943).
[14] Cohen, Crowe, and DuMond, *Fundamental Constants of Physics* (Interscience Publishers, Inc., New York, 1957).
[15] J. W. M. DuMond and E. R. Cohen, Revs. Modern Phys. 27, 363 (1955).
[16] J. O. Newton (private communication).

TABLE III. This table shows the wavelengths and energies of all nuclear lines observed during the course of the experiments described in the text.

Isotope	Natural isotopic abundance (percent)	Wavelength in Siegbahn x units	Energy in kev	Best previous value of energy	Reference
Sm^{152}	26.8	101.54±0.03	121.85±0.03	121.79 ±0.03	(cryst.)[b]
Sm^{154}	22.7	150.90±0.02	81.99±0.02	82	(scint.)[c]
Gd^{155}	14.7	206.09±0.02	60.03±0.01	60.1	(conv.)[d]
Gd^{156}	20.5	139.06±0.03	88.97±0.03	88.97 ±0.01	(cryst.)[e]
		(139.10±0.03)	(88.95±0.04)		
Gd^{157}	15.7	226.84±0.02	54.54±0.01	55	(conv.)[f]
Gd^{158}	24.9	155.61±0.02	79.51±0.02	79	(scint.)[c]
		(155.62±0.02)	(79.50±0.02)		
Gd^{160}	21.9	164.40±0.02	75.26±0.01	76	(scint.)[c]
		(164.41±0.02)	(75.25±0.02)		
Tb^{159}	100	213.36±0.02	57.99±0.01	58.0	(conv.)[d]
		155.62±0.02	79.51±0.02[a]	79	(scint.)[c]
Dy^{161}	18.9	282.30±0.02	43.83±0.01	44	(scint.)[g]
Dy^{162}	25.5	153.41±0.02	80.65±0.02	80.8	(conv.)[d]
Dy^{163}(?)	25.0	168.58±0.02	73.39±0.01	...	...
Dy^{164}	28.2	168.58±0.02	73.39±0.01	73.0	(conv.)[d]
Ho^{165}	100	130.65±0.03	94.70±0.02	94.793±0.007	(cryst.)[h]
		112.55±0.03	109.93±0.03[a]	116	(conv.)[i]
Er^{166}	33.4	153.55±0.02	80.57±0.02	80.7	(conv.)[d]
Er^{167}(?)	22.9	157.43±0.02	78.59±0.02	...	...
Er^{168}	27.1	155.04±0.02	79.80±0.02	79.9	(conv.)[d]
Er^{170}(?)	14.9	155.99±0.02	79.31±0.02	...	...
Tm^{169}	100	112.71±0.03	109.77±0.03[a]	109.78 ±0.02	(cryst.)[j]
		104.71±0.04	118.16±0.04	118.20 ±0.03	(cryst.)[j]
Yb^{171}	14.3	185.43±0.02	66.72±0.01	66.7	(conv.)[d]
		163.05±0.02	75.88±0.01	76	(p,p')[k]
Yb^{172}	21.8	157.21±0.02	78.70±0.01	78.7	(conv.)[d]
Yb^{173}	16.2	157.21±0.02	78.70±0.01	78.8	(conv.)[d]
Yb^{174}	31.8	161.81±0.02	76.46±0.01	76.6	(conv.)[d]
Yb^{176}(?)	12.7	150.65±0.02	82.13±0.02	...	...
Lu^{175}	100	108.73±0.04	113.79±0.04	113.81± 0.02	(cryst.)[j]
Hf^{176}	5.2	140.04±0.03	88.35±0.02	88.6	(conv.)[d]
Hf^{177}	18.4	109.57±0.04	112.91±0.04	112	(scint.)[c]
Hf^{178}	27.1	132.84±0.03	93.14±0.02	93.3	(conv.)[d]
Hf^{179}	13.8	100.87±0.04	122.66±0.05	123	(conv.)[i]
Hf^{180}	35.3	132.62±0.03	93.29±0.02	93.3	(conv.)[l]
Ta^{181}	100	90.89±0.04	136.12±0.06	136.25 ±0.02	(cryst.)[m]
		74.92±0.05	165.15±0.11	165	(conv.)[i]
Re^{185}	37.1	98.74±0.04	125.30±0.05	125	(conv.)[i]
Re^{187}	62.9	92.19±0.04	134.20±0.06	135	(conv.)[i]

[a] These gammas are cascade transitions.
[b] Boehm, Marmier, and DuMond (private communication).
[c] G. M. Temmer and N. P. Heydenburg, Phys. Rev. **100**, 150 (1955).
[d] Mihelich, Harmatz, and Handley, Phys. Rev. **108**, 989 (1957).
[e] F. Boehm and E. N. Hatch, Bull. Am. Phys. Soc. Ser. II, 1, 390 (1956).
[f] J. H. Bjerregard and U. Meyer-Berkhout, Z. Naturforsch. **11a**, 273 (1956).
[g] N. P. Heydenburg and G. F. Pieper, Phys. Rev. **107**, 1297 (1957).
[h] B. Andersson, Proc. Phys. Soc. (London) **A69**, 415 (1956).
[i] Huus, Bjerregard, and Elbek, Kgl. Danske Videnskab. Selskab, Mat.-fys. Medd **30**, No. 17 (1956).
[j] Hatch, Boehm, Marimer, and DuMond, Phys. Rev. **104**, 745 (1956).
[k] Elbek, Nielsen, and Olesen, Phys. Rev. **108**, 406 (1957).
[l] Mihelich, Scharff-Goldhaber, and McKeown, Phys. Rev. **94**, 794(A) (1954).
[m] F. Boehm and P. Marmier, Phys. Rev. **103**, 342 (1956).

methods. In the following paragraphs, the experimental conditions under which the remaining plates were made are discussed.

Rhenium ($Z=75$)

A rhenium metal target (30-mil Re sheet soldered to copper) was bombarded for 120 ma-hr and the two nuclear lines observed on the plate correspond to the first excited levels in the two stable isotopes, Re^{187} and Re^{185}. This element has been studied previously by electric excitation[17] with enriched isotopes and the isotopic assignment shown in Table III is unambiguous. It was not possible to observe the cascade transitions from the second excited levels, which are also excited, since this would have required an exposure time too long (~800 ma-hr) for practical consideration.

[17] McClelland, Mark, and Goodman, Phys. Rev. **97**, 1191 (1955).

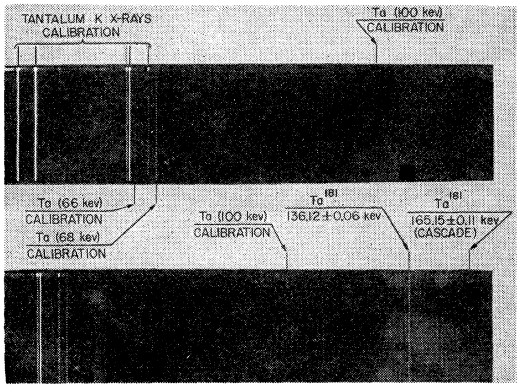

FIG. 4. X-ray and gamma-ray lines from a tantalum target bombarded for 492 ma-hr. The 165.15-kev transition is twenty times weaker then the 136.12-kev line and is therefore difficult to see on the photographic reproduction of the nuclear emulsion.

Tantalum ($Z=73$)

A tantalum metal plate was bombarded for 492 ma-hr. Two nuclear lines were visible on the plate which come from excitation of the first and second levels[17,18] in 100% abundant Ta^{181}. The 136.12-kev gamma ray corresponds to the energy of the first excited level and the line at 165.15 kev corresponds to the cascade transition between the second and first excited levels. The exposure time necessary to observe the cross-over transition is consistent with computations based on Eq. (5) and the gamma-ray yield.[2] Figure 4 shows a print of the tantalum plate.

Hafnium ($Z=72$)

A hafnium metal target ($\frac{1}{16}$-in. Hf plate soldered to copper) was bombarded for 367 ma-hr. Five nuclear lines were visible on the plate which correspond to gamma rays coming from the first excited levels of the five most abundant stable isotopes of this element

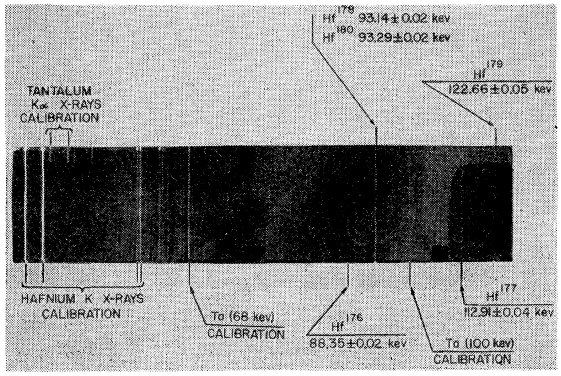

FIG. 5. X-ray and gamma-ray lines from a hafnium target bombarded for 367 ma-hr. The two lines at 93.14 kev and 93.29 kev are barely within the limit of resolution of the instrument.

[18] T. Huus and Č. Zupančič, Kgl. Danske Videnskab. Selskab, Mat.-fys. Medd. **28**, No. 1 (1953).

(Hf^{176}, Hf^{177}, Hf^{178}, Hf^{179}, and Hf^{180}). The isotopic assignment shown in Table III was made on the basis of previous electric excitation work with enriched isotopes.[17,19] One very interesting feature of this plate is the two lines from Hf^{178} and Hf^{180} at 93.14 and 93.29 kev. These lines differ in energy by about 150 ev and it can be seen in Fig. 5 that this difference is very close to the natural resolution limit of the instrument (see Sec. II for a discussion or resolution). It should also be pointed out that the isotopic assignment for these lines is not certain since the precision of previous work with separated isotopes is not high enough. The values quoted in reference 18 are 91±3 kev for Hf^{178} and 92±3 kev for Hf^{180}, so that within the accuracy of the scintillation counter work the energies are essentially equal. The isotopic assignment shown in Table III is, however, very likely, since it is in agreement with the systematics observed for the energies of the first excited levels in even-A isotopes in this region of the periodic table. Figure 5 shows a print of the hafnium plate.

TABLE IV. The gamma rays from the reaction $Cu^{65}(p,n,\gamma)Zn^{65}$ which were observed on several of the spectrographic plates are shown. The good agreement between the values obtained from the separate plates is a good indication of the validity of the method. The energies of the levels are assigned according to the decay scheme given by Bernstein and Lewis.[a]

Plate	E_1 (kev)	E_2 (kev)	E Cascade (kev)
Lu	···	115.13±0.04	···
Yb	53.92±0.01	···	···
Ho	···	115.13±0.04	61.19±0.01
Dy	···	115.10±0.04	61.20±0.01
Tb	53.92±0.01	115.13±0.04	61.19±0.01
Gd	53.92±0.01	115.05±0.04	61.20±0.01

[a] See reference 8.

Lutetium ($Z=71$)

An evaporated lutetium target (see Sec. II) was bombarded for 200 ma-hr. Two nuclear lines were clearly visible on the plate. One of these lines, at 115.13 kev, results from the reaction $Cu^{65}(p,n,\gamma)Zn^{65}$ in the copper backing (see Table IV). The other line at 113.79 kev comes from the excitation of the first level[17] in 100% abundant Lu^{175}. These levels have been observed in the decay of Yb^{175}. One of us with collaborators[20] has measured the wavelengths with the Mark I bent crystal spectrograph at The California Institute of Technology and the good agreement between their value and the present measurement is gratifying (see Table III).

Ytterbium ($Z=70$)

An evaporated ytterbium target was bombarded for 176 ma-hr. Six nuclear lines were observed on the plate and unambiguous isotopic assignments can be made

[19] N. P. Heydenburg and G. M. Temmer, Phys. Rev. **100**, 150 (1955).

[20] Hatch, Boehm, Marmier, and DuMond, Phys. Rev. **104**, 745 (1956).

for five of these lines on the basis of previous work.[21,22] The line at 78.70 kev is a double line that comes from the first excited levels in the isotopes Yb^{172} and Yb^{173}. The composite line on the plate at this energy is between 30 and 40% wider than the usual nuclear line, in addition its intensity is such that it must arise from an isotope with an abundance greater than 30%. The combined abundance of Yb^{172} and Yb^{173} is 38%. No definite isotopic assignment can be made for the gamma ray at 82.13 kev. The tentative assignment made here is that this gamma ray comes from the first excited state in 12.4% abundant Yb^{176}, since this is in qualitative agreement with the observed intensity of the line on the plate. Confirmation of this assignment must await electric excitation experiments with enriched isotopes of this material. The nuclear line at 54 kev comes from the $Cu^{65}(p,n,\gamma)Zn^{65}$ reaction in the target backing. Figure 6 shows a print of the ytterbium plate.

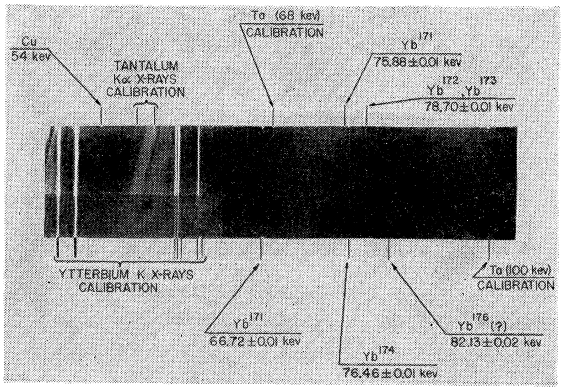

FIG. 6. X-ray and gamma-ray lines from an ytterbium target bombarded for 176 ma-hr. The line at 78.70 kev is slightly wider than other nuclear gamma-ray lines on the plate and is probably due to the superposition of gamma rays from Yb^{173} and Yb^{172}.

Thulium ($Z=69$)

An evaporated thulium target was bombarded for 100 ma-hr. Two nuclear lines were visible on the plate, one at 118.16 kev which corresponds to the transition between the second excited level and the ground state, and one at 109.77 kev which corresponds to the transition between the second and first level. A decay scheme for this isotope has been established by one of us and co-workers[20] and the present results are in good agreement with previous precision measurements of these energies. Figure 7 shows a print of the thulium plate.

Erbium ($Z=68$)

An evaporated erbium target was bombarded for 160 ma-hr. Four nuclear lines were visible on the plate and it is very probable that these gamma rays correspond to the first excited levels of the four most abundant isotopes of this material (Er^{170}, Er^{168}, Er^{167}, and

[21] Mihelich, Harmatz, and Handley, Phys. Rev. **108**, 989 (1957).
[22] Elbek, Nielsen, and Olesen, Phys. Rev. **108**, 406 (1957).

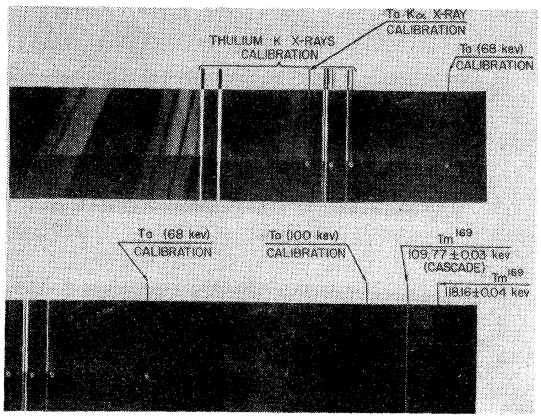

FIG. 7. X-ray and gamma-ray lines from a thulium target bombarded for 100 ma-hr. The 118.16-kev gamma ray is about 15 times less intense than the 109.77-kev line.

Er^{166}). The gamma rays at 80.57 and 79.80 kev can be assigned to Er^{166} and Er^{168}, respectively, according to a study of internal-conversion electrons emitted by these isotopes.[21] The other two gamma rays, at 78.59 and 79.31 kev, correspond to the first excited levels in Er^{167} and Er^{170}, but it is impossible with the available data to tell which gamma ray belongs to which isotope. The assignment shown in Table III is tentatively made on the basis of the observed intensities of the lines.

A print of the erbium plate is shown in Fig. 8. An interesting point is that the energies of the first excited levels in the four abundant isotopes of erbium are all within an energy range of only 1.9 kev. It will, therefore, be rather difficult to resolve the ambiguity regarding the isotopic assignment of the levels in Er^{170} and Er^{167}, even if enriched isotopes are used, unless it is possible at the same time to employ high-resolution detection methods.

Holmium ($Z=67$)

An evaporated holmium target was bombarded for 121 ma-hr. Five nuclear lines were visible on the plate. Three of these lines result from the reaction $Cu^{65}(p,n,\gamma)Zn^{65}$ in the copper backing (see Table IV). The other two lines come from excitation of the first

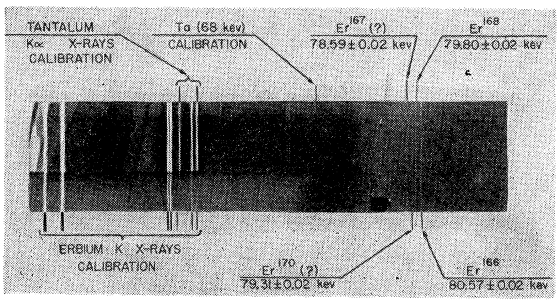

FIG. 8. X-ray and gamma-ray lines from an erbium target bombarded for 160 ma-hr.

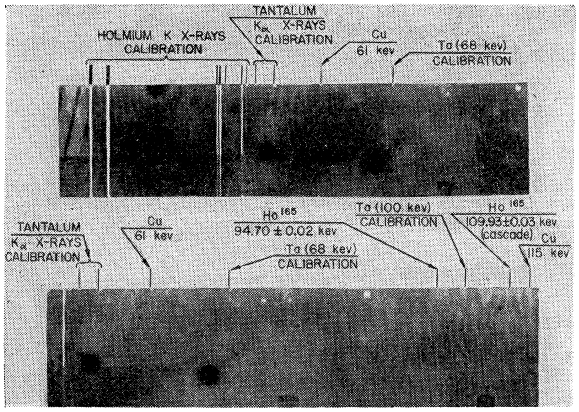

FIG. 9. X-ray and gamma-ray lines from a holmium target bombarded for 121 ma-hr. The 115-kev line from the $Cu^{65}(p,n,\gamma)Zn^{65}$ reaction is clearly visible on the plate.

two levels in 100% abundant Ho^{165}, the 94.70-kev line corresponding to the ground-state transition and the 109.93-kev line corresponding to the cascade transition between the second and first excited states.[23] A print of the holmium plate is shown in Fig. 9.

Dysprosium ($Z=66$)

An evaporated dysprosium target was bombarded for 104 ma-hr. Six nuclear lines were visible on the plate, three of which result from the $Cu^{65}(p,n,\gamma)Zn^{65}$ reaction in the target backing and the three others correspond to the excited levels in various stable isotopes of dysprosium. The isotopic assignment in Table III is made from previous work on this element by electric excitation and internal-conversion[21] experiments. The lines at 73.39 and 80.65 kev come from transitions to the first excited levels of even-A isotopes Dy^{164} and Dy^{162}. The 43.83 kev line results from excitation of the first excited level in Dy^{161}, which agrees with the work of Heydenburg and Pieper[9] and Elbek, Nielson and Oleson,[22] but is at variance with the results of Mihelich, Harmatz and Handley[21] who report a line at 25.6 kev as the first excited level in this isotope. In addition, Cork, Brice, Schmid, and Helmer[24] have given a decay scheme which is not in agreement with the assignment of the 43.83-kev line to the first excited level in Dy^{161}.

Previous electric excitation experiments also indicate that there should be a line at about 75 kev corresponding to the first excited level of Dy^{163}. The value of $\epsilon B(E2)$ quoted by Heydenburg and Pieper[7] indicates that this line should appear on the plate with an intensity about 40% of the 73.39-kev line from Dy^{164}. No such line is present on the plate. One possible explanation of this situation is that the energies of the first excited levels of Dy^{164} and Dy^{163} have precisely the same energies, so that the lines on the plate overlap. There is some evidence in favor of this suggestion since the 73.39-kev line is somewhat more intense than can be explained by using the $\epsilon B(E2)$ values given in reference 8 for either Dy^{163} or Dy^{164}. If this explanation is correct, then the two levels must be within 10 or 20 ev of each other, since no appreciable broadening of the line at 73.39 kev is observed. In Table III, a 73.39-kev level has been tentatively assigned as the first excited state in Dy^{163}. It should be pointed out that this assignment is rather uncertain since the intensity argument above is not reliable because of the strong energy dependence of the spectrograph efficiency in this energy region (see Fig. 3).

Terbium ($Z=65$)

An evaporated terbium target was bombarded for 88 ma-hr. Five nuclear lines were present on the plate, three resulting from the $Cu^{65}(p,n,\gamma)Zn^{65}$ reaction in the target backing. The other lines come from the excitation of the first two levels in 100% abundant Tb^{159}. The 57.99-kev line comes from the excitation of the first excited level and the 79.5-kev line is the cascade transition between the first and second excited levels in this isotope.[19,23]

Gadolinium ($Z=64$)

An evaporated gadolinium target was bombarded for 97 ma-hr. Six nuclear lines were visible on the plate. Three of these lines come from the $Cu^{65}(p,n,\gamma)Zn^{65}$ reaction and the other three correspond to gamma rays coming from the excitation of the first excited levels in the even-A gadolinium isotopes. The isotopic assignment in Table III is made on the basis of previous electric excitation experiments[19,25] with enriched isotopes of this element. Two other gamma rays at 55 kev and 60 kev coming from the first excited levels in Gd^{157} and Gd^{155} should also be visible on the plate. These lines should be somewhat weaker than those arising from the even-A isotopes, since odd-A isotopes are somewhat less abundant and the $\epsilon B(E2)$ values for these levels are considerably smaller than those for the levels in the even-A isotopes.[2] Since the gadolinium plate was quite dark because of the rather large neutron background from the copper target backing, it is not surprising that these lines were not visible on the plate.

A separate experiment to observe the gamma rays from the odd-A isotopes was performed by operating the accelerator at 1.8 Mev. This can be done by using only the first of the two accelerating vessels. At this energy, no neutrons are produced in the copper target since the $Cu^{65}(p,n,\gamma)Zn^{65}$ threshold is at 2 Mev, so that the nuclear emulsion was quite clear when developed at the end of the run. On the other hand, the gamma-ray yield at 1.8 Mev is considerably smaller than at 3.7 Mev, and hence an exposure time of 418 ma-hr was

[23] Huus, Bjerregard, and Elbek, Kgl. Danske Videnskab. Selskab, Mat.-fys. Medd. **30**, No. 17 (1956).
[24] Cork, Brice, Schmid, and Helmer, Phys. Rev. **104**, 481 (1956).
[25] H. Mark and G. T. Paulissen, Phys. Rev. **100**, 813 (1955).

necessary to observe the lines. Five nuclear lines were observed on this plate, three from excited levels in the even-A isotopes, which are also observed on the plate made at 3.7 Mev, and two others which arise from the excitation of the first excited levels in the odd-A isotopes.[2,19] The energies for excited levels in the gadolinium isotopes shown in Table III are taken from the 1.8-Mev plate. The energies shown in parentheses for the even-A isotopes are computed from the plate made at full proton energy. The good agreement between these values is an additional confirmation of the reliability of the method.

It should be pointed out that, in general, it was not found economical or necessary to make exposures at half energy for other materials in order to increase the signal-to-noise ratio. Usually, the layer of material evaporated on the copper was thick enough to prevent bothersome neutron background effects. In addition, the lower gamma-ray yield at the smaller proton energy made it necessary to raise exposure times by a factor of 3 or 4 which makes such experiments very costly in operating time.

Samarium ($Z=62$)

An evaporated samarium target was bombarded for 100 ma-hr. Two nuclear lines were visible on the plate, the line at 81.99 kev coming from the first excited level in Sm^{154} and the line at 121.85 kev coming from excitation of the first level in Sm^{152}. The isotopic assignments are made on the basis of previous work with enriched isotopes.[19,25] The gamma rays of 335 and 500 kev coming from the other abundant even-A isotopes (Sm^{150} and Sm^{148}) were not observed because of their high energy which makes detection very difficult (see Fig. 3). A precision measurement of the 121.85-kev level in Sm^{152} has been made by Boehm and Hatch[26] and their result is in fairly good agreement with the value listed in Table III. Figure 10 shows a print of the samarium plate.

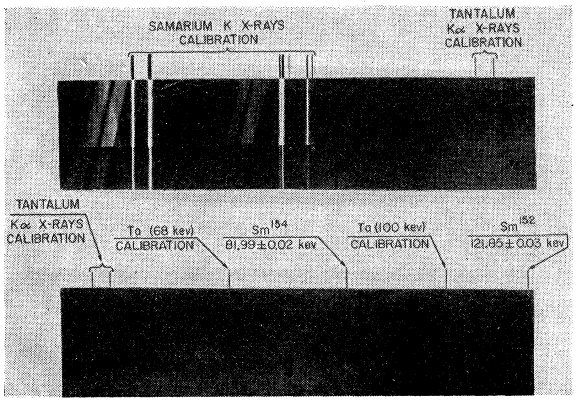

FIG. 10. X-ray and gamma-ray lines from a samarium target bombarded for 100 ma-hr.

[26] F. Boehm and E. N. Hatch (private communication).

V. DISCUSSION OF RESULTS

Before discussing the possible theoretical implications of the measurements presented in the previous section it is important to ask how closely the energies listed in Table III are related to the energies of the excited levels in the corresponding isotopes. Two possible effects that may cause a Doppler shift and thus change the energy of the gamma ray are the recoil motion of the nucleus when the gamma ray is emitted and the recoil motion of the nucleus caused by the collision with the incoming proton. The first effect lowers the measured energy of the gamma ray by:

$$\Delta E = E_\gamma^2/Mc^2, \tag{8}$$

where E_γ is the energy of the emitted gamma ray and Mc^2 the rest energy of the nucleus. For most transitions ($\sim$0.1 Mev) in the isotopes considered ($A\sim150$) this energy shift is of the order of 0.10 ev which is about 300 times smaller than the standard deviations quoted in Table III. The recoil of the nucleus due to collisions will tend to broaden the observed spectral lines and also to shift them because gamma rays emitted at the spectrograph angle ($\sim30°$) will tend to be preferentially associated with certain recoil directions. The maximum energy shift expected from proton recoil effect is:

$$\Delta E \approx (\beta/A)E_\gamma, \tag{9}$$

where A is the atomic weight, β is the v/c of the incoming proton, and E_γ is again the energy of the transition. The value of ΔE computed from Eq. (9) for most cases of interest is of the order of 100 ev which is of the same order or somewhat larger than the standard deviation. The actual energy shift is of course much smaller since Eq. (9) assumes that all the momentum of the incoming proton is transferred to the target nucleus and also that the target nucleus is still in motion when the gamma ray is emitted. Both of these assumptions are wrong, particularly the latter since the half-lives of most of these transitions are much larger ($\sim10^{-10}$ sec) than the time taken by the recoiling nucleus to come to rest in the lattice of the target material ($\sim10^{-14}$ sec). It can therefore be concluded that the gamma-ray energies given in Table III are equal (within the quoted standard deviation) to the excitation energies of the corresponding isotopes.

All the energy levels listed in Table III belong to the class of nuclear rotational levels that has been extensively treated in the theoretical literature.[5] Rotational levels possess two distinguishing features: One is that they have radiative transition probabilities which are larger by one or two orders of magnitude than those expected from the transitions of a single nucleon. The other is that the spectra obey interval rules which are similar to those employed in the description of a diatomic molecule. For even-A isotopes,

$$E = (\hbar^2/2\mathcal{I})I(I+1), \tag{10}$$

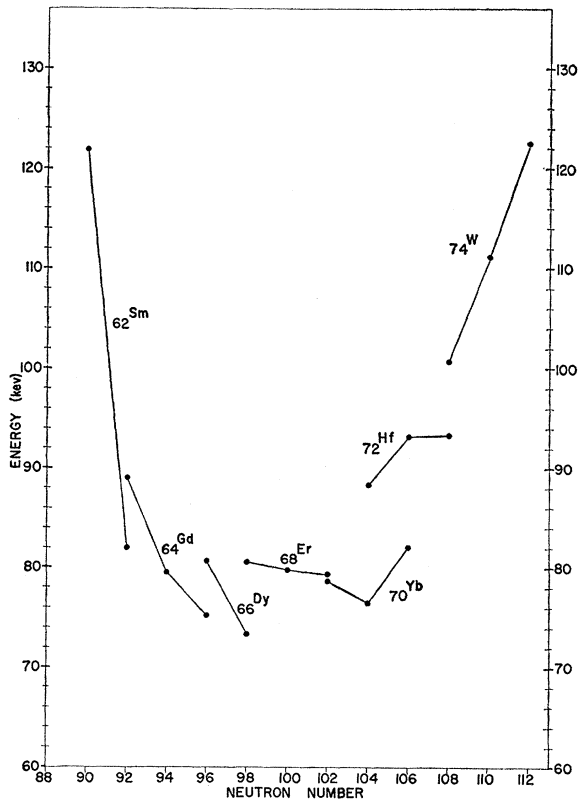

FIG. 11. Energies of first excited levels in even-A isotopes as a function of neutron number.

where E is the energy of the level, I the spin, and $\mathcal{I}$ the moment of inertia. The spin sequence in even-A isotopes is $I=0, 2, 4, 6$, etc. For odd-A isotopes with ground-state spin $I_0=\frac{1}{2}$:

$$E=\frac{\hbar^2}{2\mathcal{I}}[I(I+1)-I_0(I_0+1)], \tag{11}$$

where the spin sequence is I, I_0+1, I_0+2, I_0+3, etc. If $I_0=\frac{1}{2}$, then an additional term appears in Eq. (11) which arises from the term in the Hamiltonian containing the products $\mathbf{I}\cdot\mathbf{j}$. ($\mathbf{I}$ is the total angular momentum and $\mathbf{j}$ is the single-particle angular momentum.) In an axially symmetric nucleus, this term has diagonal matrix elements only if $I_0=j=\frac{1}{2}$ and has the form:

$$E=\frac{\hbar^2}{2\mathcal{I}}[a(-1)^{I+\frac{1}{2}}(I+\tfrac{1}{2})]. \tag{12}$$

The rotational spectrum for an odd-A nucleus with $I_0=\frac{1}{2}$ is therefore determined by two parameters: the momentum of inertia, $\mathcal{I}$, and the decoupling parameter, a, the latter of which depends on the wave function of the intrinsic particle motion in the ground state. This wave function will be a linear combination of states with $\Omega=+\frac{1}{2}$ and $-\frac{1}{2}$ (Ω is the projection of j on the nuclear symmetry axis) which are degenerate due to the axial symmetry of the nucleus. The decoupling parameter, a, is determined by the coefficients of the terms in this linear combination.

In even-A isotopes, only the first excited (2^+) levels can be studied by electric excitation, since the cross sections for the excitation of levels with multipolarities higher than electric quadrupole are too small. It is not possible therefore to verify the rotational interval rule (10) in a given isotope. However, it is of some interest to study the behavior of the first excited levels in even-A nuclei as a function of the neutron and/or proton number.[27,28] Figure 11 shows the rotational energy parameter as a function of neutron number for all the even-A isotopes listed in Table III. (The data for W^{182}, W^{184}, W^{186} are taken from reference 1). This figure shows features very similar to previous figures of this type given in references 27 and 28. The somewhat better resolution of the present experiments reveals some interesting fine structure on such curves. For example, there appear to be two points ($Z=70$, $N=104$; and $Z=66$, $N=98$) for which the energy curve has a "minimum." Another feature is that the isotopes Hf^{178} and Hf^{180} have their first excited levels at almost precisely the same energy, which means that the 107th and 108th neutrons are added in such quantum states that they apparently make no contribution to the moment of inertia.

In odd-A isotopes, the spin change between successive rotational states is one unit and it is therefore possible to reach the first two rotational levels by electric quadrupole excitation. In Yb^{171} two gamma rays corresponding to the transitions between the first and second excited levels and the ground state were observed. In Tm^{169}, the transition from the second excited level to the ground state and the cascade transition from the second level to the first were observed. In Ta^{181}, Ho^{165}, and Tb^{159} the transitions between the first level and the ground state and the cascade transitions between the second and first excited levels were observed. In the remaining odd-A isotopes listed in Table III only one gamma ray corresponding to the first excited level was observed.

For the isotopes in which two gamma rays are observed, the energies of the first and second levels can be deduced from the decay schemes. The isotopes Ta^{181},

TABLE V. Rotational spectra of odd-A isotopes with $I_0\neq\frac{1}{2}$. The difference between the computed and measured energy of the second level is shown in column six.

Isotopes	I_0	E_1(kev)	E_2(kev), exp.	E_2(kev), theo.	ΔE(kev)
$_{65}Tb^{159}$	3/2	57.99±0.01	137.50±0.02	139.18±0.02	−1.68±0.03
$_{67}Ho^{165}$	7/2	94.70±0.03	204.63±0.04	210.44±0.07	−5.81±0.08
$_{73}Ta^{181}$	7/2	136.12±0.06	301.27±0.12	302.49±0.13	−1.22±0.18

[27] G. Scharff-Goldhaber and J. Weneser, Phys. Rev. **98**, 212 (1955).
[28] G. Scharff-Goldhaber, Phys. Rev. **103**, 837 (1956).

TABLE VI. Rotational energy parameters in odd-A isotopes.

Isotope	Ground-state spin	$3\hbar^2/\mathcal{I}$ in kev	Decoupling parameter[a]
Gd^{155}	3/2[a]	72.04±0.01	···
Gd^{157}	3/2[a]	65.54±0.01	···
Tb^{159}	3/2[a]	69.59±0.01	···
Dy^{161}	5/2[b]	37.57±0.01	···
Dy^{163}	5/2[b]	62.90±0.01	···
Ho^{165}	7/2[a]	63.13±0.01	···
Er^{167}	7/2[c]	52.39±0.01	···
Tm^{169}	1/2[a]	74.27±0.02	−0.7740
Yb^{171}	1/2[d]	72.22±0.02	0.8478
Yb^{173}	5/2[d]	67.45±0.01	···
Lu^{175}	7/2[a]	75.86±0.02	···
Hf^{177}	7/2[a]	75.28±0.02	···
Hf^{179}	9/2[a]	66.90±0.01	···
Ta^{181}	7/2[a]	90.75±0.03	···
Re^{185}	5/2[a]	107.39±0.04	···
Re^{187}	5/2[a]	115.03±0.04	···

[a] See reference 2.
[b] See reference 6.
[c] B. Bleany and H. E. D. Scoville, Proc. Phys. Soc. (London) **A64**, 204 (1951).
[d] A. H. Cooke and J. G. Park, Proc. Phys. Soc. (London) **A69**, 282 (1956).

Ho^{165}, and Tb^{159} have ground-state spins larger than $\frac{1}{2}$ and therefore the level sequence should be given by Eq. (11). Since Eq. (11) contains only one parameter, $\mathcal{I}$, which is fixed by the energy of the first level, the energy of the second level can be predicted with a precision comparable to the precision with which the energy of the first is measured. This value can then be compared with the measured energy of the second level. From the results listed in Table V it can be seen that in each case the measured energy of the second level is slightly smaller than the prediction made using Eq. (11). There are two effects that might account for the observed deviations from Eq. (11). One is a "rotation-vibration" interaction of the type encountered in molecular spectroscopy, which results from an increase in the moment of inertia as the excitation energy is raised. This effect always depresses the energy of the second level and is of the order $E_{\text{rot}}^3/E_{\text{vib}}^2$. The second perturbation that changes the energy of the second rotational level is the rotation-particle coupling which has been discussed by Kerman[29] for the case of W^{183}. This deviation arises from the same $\mathbf{I}\cdot\mathbf{j}$ terms in the Hamiltonian that cause the anomalous rotational spectrum (12) for $I_0=\frac{1}{2}$ nuclei, and is due to the presence of intrinsic (i.e., particle) excited levels near the ground state which perturb its rotational band. The rotation-particle coupling can either depress or raise the energy of the second level and the direction and magnitude of the effect depends in detail on the properties of the perturbing single-particle states. The order of magnitude of the rotation-particle coupling is $E_{\text{rot}}^3/(E_0-E_1)^2$, where (E_0-E_1) is the energy difference between the ground state and the first single-particle level.

It is evident from the foregoing discussion that it is not possible to distinguish clearly which of the two effects considered is more important in causing the observed deviations from Eq. (11) since both perturbations give rise to energy deviations of about the same order of magnitude. Further theoretical work should be done on Ta^{181} since there is a single-particle level at 482 kev[30] that could perturb the rotational spectrum of the ground state.

Table VI also shows the rotational energy parameters for all the odd-A nuclei considered here together with the decoupling parameters for the odd-A $I_0=\frac{1}{2}$ isotopes. (For the $I_0=\frac{1}{2}$ isotopes, no check of the rotational sequence can be made since the first two levels only serve to define the two parameters a and $\mathcal{I}$.) The values of $3\hbar^2/\mathcal{I}$ for first excited levels in odd-A isotopes tend to be somewhat lower than the corresponding numbers in neighboring even-A isotopes. This effect can also be explained by assuming that rotation-particle coupling is an important perturbation.

VI. ACKNOWLEDGMENTS

A great many people contributed to the successful conclusion of this work. Among them were Professor F. H. Spedding of Iowa State College, who supplied all the rare-earth samples; Dr. R. S. White, A. J. Oliver and G. R. Leipelt of UCRL, Livermore, who processed the nuclear emulsions; Daniel O'Connell of UCRL, Berkeley, who developed the techniques for evaporating the rare earths; Jack Matthews, who wrote the programs for the IBM-650 computations; and the A-48 crew members, headed by P. V. Livdahl and D. H. Birdsall, who made many valuable contributions during the course of the experiments. In addition, the authors wish to thank Dr. Arnold Clark for his help and Dr. C. M. Van Atta and Dr. H. F. York for their continued support of this work.

[29] A. K. Kerman, Kgl. Danske Videnskab. Selskab Mat.-fys. Medd. **30**, No. 15 (1956).

[30] P. H. Stelson and F. K. McGowan, Phys. Rev. **105**, 1346 (1956).

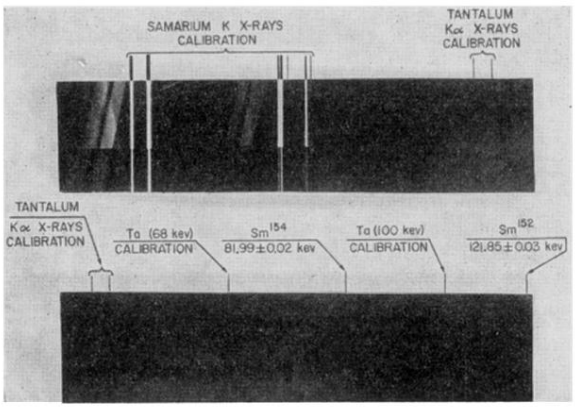

FIG. 10. X-ray and gamma-ray lines from a samarium target bombarded for 100 ma-hr.

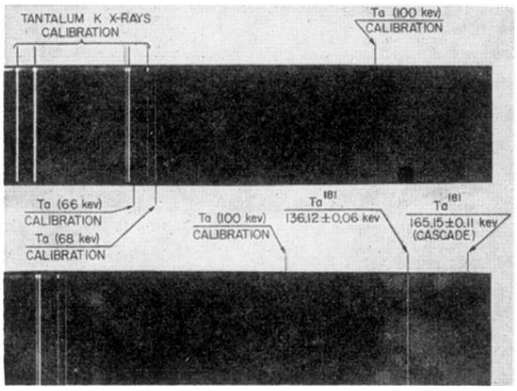

FIG. 4. X-ray and gamma-ray lines from a tantalum target bombarded for 492 ma-hr. The 165.15-kev transition is twenty times weaker then the 136.12-kev line and is therefore difficult to see on the photographic reproduction of the nuclear emulsion.

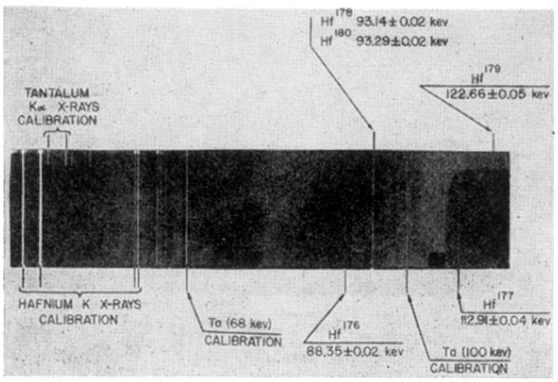

FIG. 5. X-ray and gamma-ray lines from a hafnium target bombarded for 367 ma-hr. The two lines at 93.14 kev and 93.29 kev are barely within the limit of resolution of the instrument.

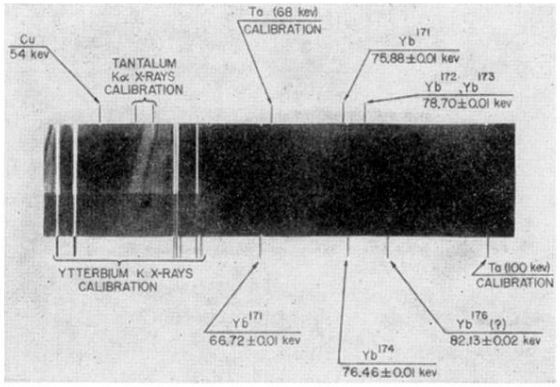

FIG. 6. X-ray and gamma-ray lines from an ytterbium target bombarded for 176 ma-hr. The line at 78.70 kev is slightly wider than other nuclear gamma-ray lines on the plate and is probably due to the superposition of gamma rays from Yb^{173} and Yb^{172}.

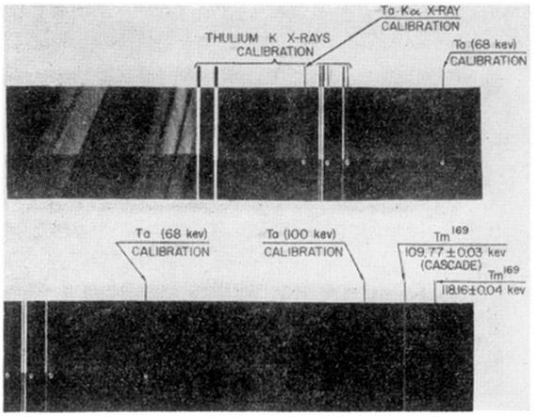

FIG. 7. X-ray and gamma-ray lines from a thulium target bombarded for 100 ma-hr. The 118.16-kev gamma ray is about 15 times less intense than the 109.77-kev line.

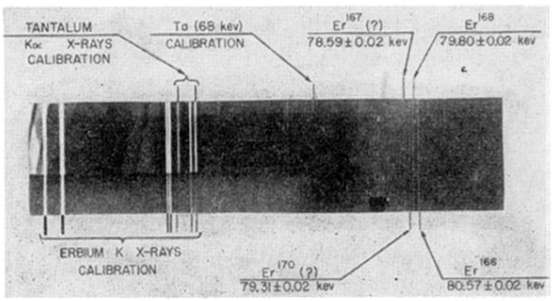

FIG. 8. X-ray and gamma-ray lines from an erbium target bombarded for 160 ma-hr.

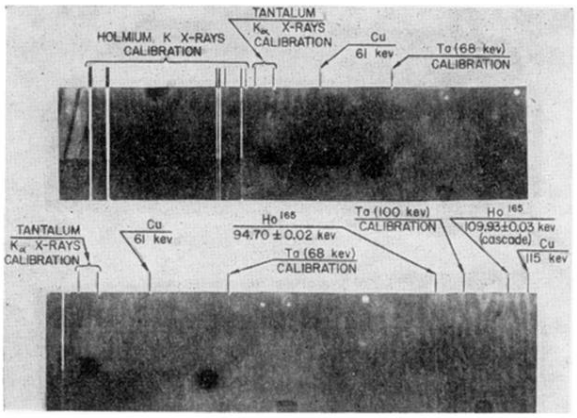

FIG. 9. X-ray and gamma-ray lines from a holmium target bombarded for 121 ma-hr. The 115-kev line from the $Cu^{65}(p,n,\gamma)Zn^{65}$ reaction is clearly visible on the plate.